DFT and Local MP2 Study of Switching Process in a pH Controllable Molecular "Shuttle"

SERGUEI FOMINE, PATRICIA GUADARRAMA, MIKHAIL ZOLOTUKHIN

Instituto de Investigaciones en Materiales, Universidad Nacional Autónoma de México, Apartado Postal 70-360, CU, Coyoacán DF 04510, México

Received 11 May 2006; Accepted 10 July 2006
Published online 3 October 2006 in Wiley InterScience (www.interscience.wiley.com).
DOI 10.1002/qua.21206

ABSTRACT: A pH controllable molecular "shuttle," comprising of dibenzo[24]crown-8 (DB24C8) macroring bound to a "finger" molecule possessing two different recognition sites has been studied at the density functional theory (DFT) and Møller-Plesset second-order (MP2) levels of theory. The calculation confirmed experimental results that translational conformer with DB24C8 located around NH_2^+ station has the lowest energy, while the conformer with DB24C8 located around NH station shows the highest energy. It has been found that Bpym2+ unit consists of two "substations" separated by an energy barrier of 3–17 kcal/mol depending on the state of the NH–NH_2^+ station. The translational conformers are stabilized by NH···O, $^+$NH···O, $^+$NCH···OH-bonds, and π–π stacking with different contributions, depending on the conformer type. © 2006 Wiley Periodicals, Inc. Int J Quantum Chem 107: 685–693, 2007

Key words: molecular shuttle; binding energy; DFT; computational study; LMP2

Introduction

Rotaxanes are molecular assemblies that are mechanically linked but chemically independent [1]. A typical system consists of two components, a ring molecule threaded by a dumbbell-shaped molecule. In a rotaxane, the bulky ends of the dumbbell-shaped component prevent spontaneous unthreading of the ring. If the ring can be forced to move from one initially favored "station" on the dumbbell to a second one as a consequence of some external stimulus, a very basic molecular shuttle has been produced, with the external stimulus changing the preferential binding site. An example of an acid–base controllable molecular shuttle in which the rotaxane bears a

Correspondence to: S. Fomine; e-mail: fomine@servidor.unam.mx
Contract grant sponsor: DGAPA.
Contract grant number: IX-100902/14.

fluorescent and redox-active anthracene stopper unit in addition to a dialkylammonium center and a Bpym2+ unit has been reported by Stoddart and coworkers [2].

Upon the addition of an appropriate base, the NH_2^+ group is deprotonated and the crown ether switches from the NH center to the $Bpym^{2+}$. Treatment with acid restores the NH_2^+ center and reverses the processes. Using the anthracene stopper, it is possible to monitor the switching process by means of an electrochemical and photophysical techniques due to its absorption, luminescence, and redox properties. The switching process in molecular "shuttles" has been a subject of a number molecular mechanic studies [3–6]. However, to the best of our knowledge, there is only one quantum mechanic (semiempirical) study [7] of a pH-switchable [2] rotaxane-based molecular "shuttle" with two 3,5-(di-ter-butyl)phenyl stoppers, which is related to the size of the system involved in quantum mechanical treatment. The process of switching between neutral and protonated states of this complex has been studied and although semiempirical model correctly predicts the most important features of the switching process this model is too simple to give deep insight into the nature of intermolecular interactions. Another approach [8] was used to understand the nature of interaction in paraquat-based catenanes and rotaxanes. In that work, a small model system was used consisting of methylpyridinium ion and dimethylether representing a model for the interaction between paraquat cycle and a polyethyleneoxide chain. The model system was studied at the Møller–Plesset second-order (MP2)/6-311++G** level, and the importance of CH···O hydrogen bonds between charged system and oxyethylene chain was shown. In a recent paper [9], we described a theoretical study of the interactions in dibenzo[24]crown-8 (DB24C8)–*n*-dibutylammonium (DBM)–pseudo-rotaxane at density functional theory (DFT) and MP2 levels. It has been shown that the use of hybrid BHandHLYP functional for the geometry optimization and local implementation of MP2 theory for single-point energy evaluation reproduces experimental binding energy in pseudo-rotaxane very well. Moreover, a fast pseudo-spectral integral evaluation technique implemented in Jaguar suite of programs [10] makes it possible to study a full size molecular switch at DFT or correlated ab initio levels. Therefore, the goal of this study is to obtain deeper insight into the nature of interactions in a pH controllable molecular "shuttle" using DFT and ab initio correlated methods.

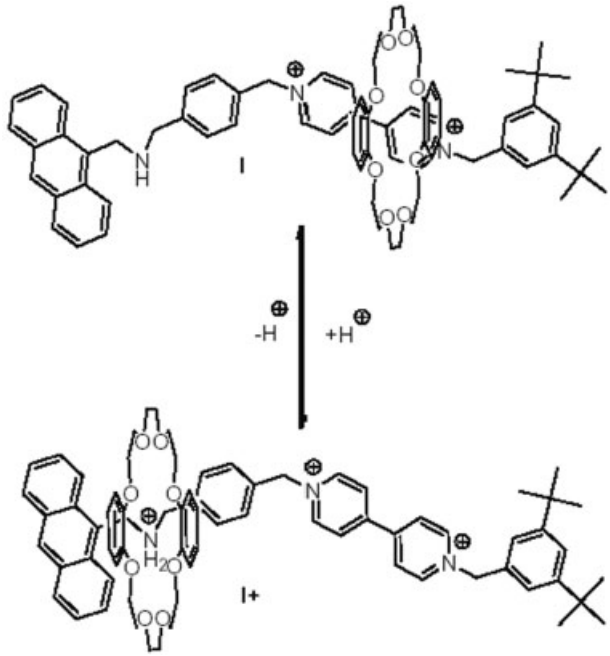

SCHEME 1. Shuttling process in molecular "shuttle" I reported by Stoddart and colleagues [2].

Computational Details

The translational isomerism of molecular shuttle **I** (Scheme 1) has been studied. First, successive conformational search of protonated and deprotonated forms of molecular shuttle **I** was carried out using a Monte Carlo (MC) torsional sampling algorithm incorporated in the Macromodel 9.0 suite of prpgrams, using the OPLS-AA force field in the gas phase. Each conformational search included 10,000 iterations. Five lowest-energy translational conformers of each type (**Ib**, **Ic**, **Ia**+, **Ib**+, and **Ic**+) were used for further selection by single-point energy calculation at the local MP2 level of theory, using a standard 6-31G* basis set (LMP2/6-31G* model) followed by a single-point salvation energy calculation at BHandHLYP/6-31G* level in acetone solution using the Poisson–Boltzmann method implemented in the Jaguar 6.0 suite of programs. The geometry of deprotonated structure **Ia**, was generated by removing one proton from the **Ia**+ structure. The local MP2 approach was shown to have some advantages compared with the canonical MP2

method in studying intermolecular complexes [11]; moreover, the LMP2 method gives reliable results in describing hydrogen bonds at substantially lower computational cost than canonical MP2 [12, 13]. A detailed description of the LMP2 approach is given in Ref. [13]. The lowest-energy conformers of each type were selected based on LMP2 and BHandHLYP/6-31G* solvation energies calculations and used for further geometry optimizations. Low-energy conformers were fully optimized using a hybrid BHandHLYP functional and a standard 6-31G* basis set (BHandHLYP/6-31G* model). To calculate the binding energies of DB24C8 and the dumbbell-shaped molecule in molecular "shuttle," the first lowest-energy conformations of DB24C8 and a "fingers" (protonated and deprotonated) have been located, used Macromodel 9.0 software with a MC torsional sampling algorithm. Conformational search has been run until no new lowest-energy conformer is located. The lowest-energy conformers were optimized at BHandHLYP/6-31G* level of theory. After the optimizations were converged, a single-point energy evaluations of BHandHLYP optimized structures was carried out at LMP2/6-31G* level. It was recently shown that BHandHLYP/6-311++G** and MP2/6-311++G** models perform exceptionally well for binding energies of crown ether–ammonium complexes [9].

To estimate the activation energies of translational isomerism, the transition states search was carried out using quadratic synchronous transit method included in the Jaguar 6.0 suite of program. Owing to the size of the job (nearly 1,500 basis functions), no frequency jobs were run, therefore, located structures might not be representing true transition states, however, the visual analysis of the geometry show that their structures connect two lowest-energy conformers giving at least semiquantitative values for the activation energies. The solvent effect on the binding energy was studied at BHandHLYP/6-31G* level with Poisson–Boltzmann method [14, 15] implemented in the Jaguar 6.0 suite of programs, which represents one of the modifications of continuum model. The structures have not been reoptimized in the presence of solvent, since it has been shown previously that reoptimization has a very limited effect on the computed energies [16–20]. Nevertheless, a test calculation for **Ic** has been carried out to verify the influence on total geometry optimization in solution on the calculated solvation energy. For gas phase and solution phase optimized geometries, the calculated solvation energies at BHandHLYP/6-31G* level were found to be of −115.0 and −116.2 kcal/mol, respectively, representing the error of 1.2 kcal/mol, which is well within the method error. All DFT geometry optimizations and single-point energy evaluation were carried out using Jaguar 6.0 suite of programs.

Results and Discussion

Figures 1 and 2 show BHandHLYP/6-31G* optimized geometries of the located lowest-energy conformers of protonated and deprotonated forms of molecular shuttle **I** corresponding to the different binding sites. In conformer **Ia**+, the crown ether is bound to ammonium group while in conformers **Ib**+ and **Ic**+ crown ether fragment is linked to Bpym2+ unit. As shown in Figures 1 and 2, all six conformers manifest π–π stacking interactions as followed from parallel positions of aromatic fragments in the dumbbell-shaped component and crown ether. X-ray structure of protonated form of the molecular "shuttle" is quite similar to that of **Ia**+ with π–π stacking involved anthracene fragment. Absorption/emission experiments in solution [2] show evidence of interaction between DB24C8 with anthracene fragment (quenching of the crown ether's fluorescent dioxybenzene by nearby anthracene moiety), thus validating the computational method.

The nature of intermolecular interactions in a complex can be understood analyzing its geometry. Table I shows the shortest O—H distances between oxygen atoms of crown ether and hydrogens linked to nitrogen atoms or to carbon atoms adjacent to nitrogen for the located translational conformers.

It has been shown both theoretically [9] and experimentally [21] that complexes of secondary ammonium ions and crown ethers are stabilized mainly due to NH···O and CH···O interactions where CH···O binding represents up to 25% of total interaction energies in the case of aliphatic ammonium ions. As shown in Table I, conformer **Ia**+ is stabilized by NH···O and CH···OH interactions. In conformers **Ib**+ and **Ic**+, the stabilization is achieved due to H-bonding between DB24C8 oxygens and CH_2N^+ and o-protons of $Bpym^{2+}$ unit. In the case of deprotonated molecular "shuttle," conformers **Ib** and **Ic** are stabilized due to H-bonding between DB24C8 oxygens and CH_2N^+ and aromatic protons of the $Bpym^{2+}$ unit, similarly to protonated species **Ib**+ and **Ic**+, while the stabilization of **Ia** is due to NH···O interactions. It is

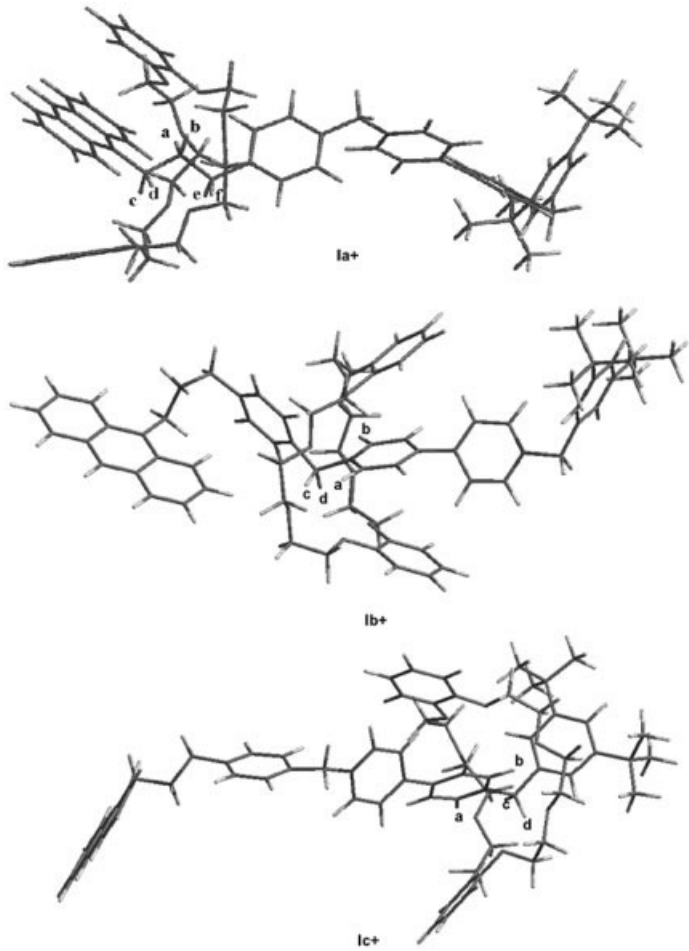

FIGURE 1. BHandHLYP/6-31G* optimized geometries of the located lowest-energy conformers of protonated forms of molecular shuttle I.

noteworthy that, as mentioned above, all conformers are stabilized by $\pi-\pi$ stacking interactions as well. Thus, in the case of protonated conformers (**Ia**+, **Ib**+ and **Ic**+), the lowest-energy structures are extended ones due to electrostatic repulsion of two cationic centers and $\pi-\pi$ stacking interactions are manifested only between catechol of DB24C8 and "finger" molecules, while in the case of the deprotonated form **Ic** the lowest-energy conformer is a folded one in which $\pi-\pi$ stacking involves three phenyl rings and anthracene group. It is noteworthy [2] that deprotonation of "shuttle" molecule with *i*-Pr_2NEt or Bu_3N leads to the appearance of yellow coloring c, indicating charge transfer (CT) interactions between DB24C8 catechol rings and the $Bpym^{2+}$ dication. This observation is in very good agreement with the lowest-energy structure of deprotonated "shuttle" (**Ic**), where catechol ring is located very close to the pyridinium fragment of $Bpym^{2+}$ unit (interplane distance is ~3.3 Å) allowing for CT interactions. Natural bond orbital (NBO) analysis of the CT interaction in **Ic** using second order perturbation analysis of Fock matrix in the NBO basis at the BHandHLYP/6-31G* level of theory reveals CT interactions between DB24C8 (donor) and $Bpym^{2+}$ unit (acceptor). The most important CT interactions involves DB24C8 oxygen lone pairs transfer to N—H and C—H antibond orbitals of the $Bpym^{2+}$ unit and catechol π electrons transfer to antibond π-orbitals of $Bpym^{2+}$ fragment. A total charge transfer in **Ic** is of 0.11 e in the gas phase. Similar charge transfer is found when salvation is taken into account.

Figure 3 depicts relative energies of conformers in acetone solution. As seen in the case of protonated form the lowest-energy conformer is **Ia**+ in

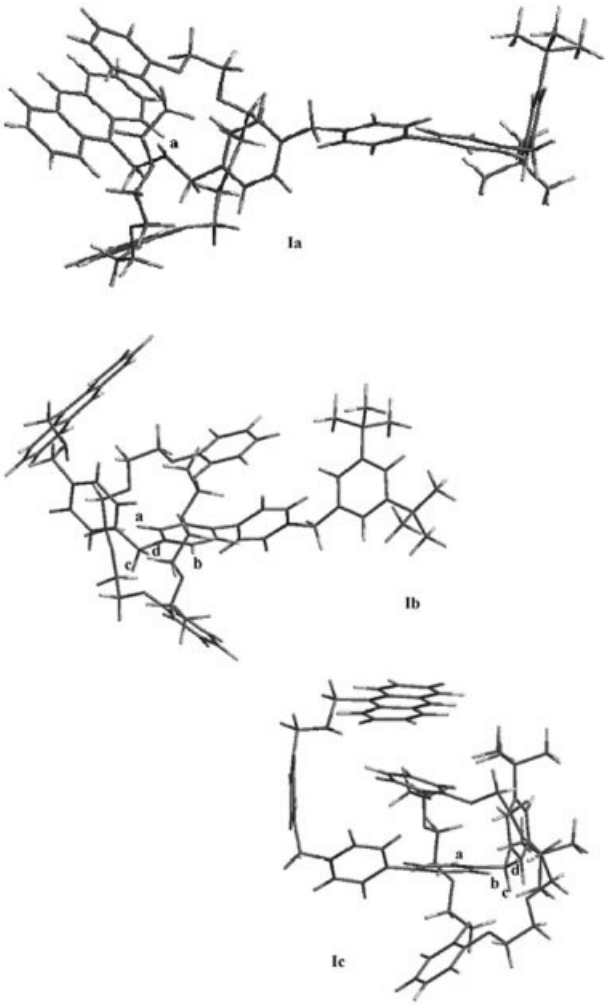

FIGURE 2. BHandHLYP/6-31G* optimized geometries of the located lowest-energy conformers of deprotonated forms of molecular shuttle I.

agreement with experimental finding [2]. In the case of the deprotonated structure, the NH recognition site gives the conformer with the highest energy, forcing the crown ether ring migrate to $Bpym^{2+}$ station in accordance with experimental observations. The energy profile shows two important features. First, the $Bpym^{2+}$ station has two distinct binding sites associated with positively charged nitrogen atoms separated by an energy barrier. Therefore, $Bpym^{2+}$ station is composed of two substations. On the first inspection this result clashes with the spectroscopic results reported by Stoddart [2]. ^{1}H-NMR on I were reported to show broadening below 233 K, but "no supplementary sets of resonance, for any other translational isomers are evident." This fact can be interpreted as that at room temperature ^{1}H-NMR spectra were at fast exchange limit and that coalescence occurred below 233K, which agrees very well with the barrier of 8 kcal/mol found between "substations"(Fig. 3). Thus, the existence of two binding regions for DB24C8 crown ether allows explaining experimentally observed broadening of ^{1}H-NMR spectra below 233 K.

Second, the relative energies of two pyridinium substations depend on the ammonium-amine station state, which is an example of mutual influence of stations in the molecular "shuttle." As shown in Figure 3, conformer **Ib**+ is more stable than **Ic**+, while conformer **Ic** is more stable compared with **Ib**. It seems that inductive effect originated by ammonium station increase electrostatic interactions at the pyridinium substation closest to the ammonium group.

TABLE I

Selected shortest H—O distances (Å) of translational isomers in molecular "shuttle" I shown in Figs. 1 and 2.*

	Ia+
O—H_a	1.93
O—H_b	1.87
O—H_c	2.26
O—H_d	2.42
O—H_e	2.53
O—H_f	2.55
	Ib+
O—H_a	2.05
O—H_b	2.32
O—H_c	2.07
O—H_d	2.42
	Ic+
O—H_a	2.00
O—H_b	2.14
O—H_c	2.20
O—H_d	2.33
	Ia
O—H_a	2.19
	Ib
O—H_a	2.23
O—H_b	2.03
O—H_c	2.28
O—H_d	2.30
	Ic
O—H_a	2.09
O—H_b	2.10
O—H_c	2.50
O—H_d	2.44

* Experimental values from Ref. [2].

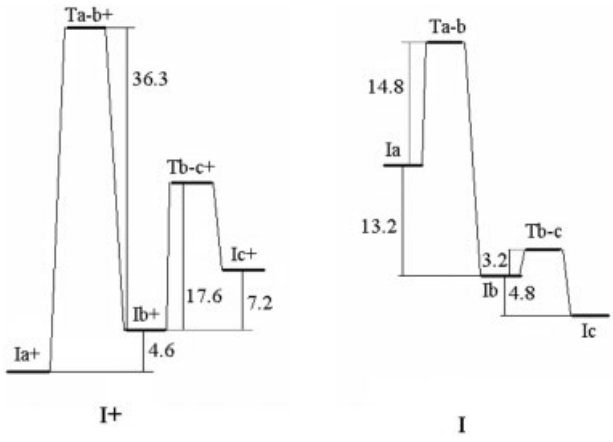

FIGURE 3. Energy profile (kcal/mol) for the shuttling process in molecular shuttle I in acetone solution calculated at LMP2/6-31G*//BHandHLYP/6-31G* level of theory (kcal/mol).

In the deprotonated state, the most stable state of molecular "shuttle" is **Ic** and the activation energy separating **Ic** and **Ib** conformer is of 8 kcal/mol in acetone solution. According to ^{1}H-NMR study [2], the deprotonated molecule is asymmetrically coordinated to the $Bpym^{2+}$ station supporting the hypothesis that **Ic** is global minimum for deprotonated "shuttle."

Once the "shuttle is protonated, the relative stability of $Bpym^{2+}$ station is changed and the most stable state becomes **Ia**+. To reach the state **Ia**, two activation barriers should be overcome as shown in Figure 3. The highest one is due to transition from state **Ib**+ to **Ia**+ .Deprotonation of molecular "shuttle" results in formation of conformer **Ia**, which is transformed into **Ic** passing two energetic barriers. As shown in the calculations, the activation energies of **Ia** to **Ic** process is lower compared with **Ic**+ to **Ia**+ that should be reflected in faster process **Ia** to**Ic** compared with the **Ic**+ to **Ia**+ one. Figure 4 shows located "transitions states" for shuttling process. As shown in all the located structures, the crown ether ring is situated between two stations.

To obtain better insight into the nature of binding in molecular "shuttle" I. the binding energies in molecular "shuttle" have been calculated. Table II shows gas and solution phase binding energies of different translational conformers calculated at correlated LMP2 as well as at HF levels.

The difference between HF and LMP2 binding energy represents the correlation stabilization having to do with the dispersion stabilization interaction [22]. Table II shows that binding energies are in line with the stabilities of conformers. Thus, the highest binding energy is for the most stable conformer **Ia**+ and the lowest one for **Ia**. Similar to relative stability of the translational conformers the binding energy of **Ib**+ is higher than **Ic**+ and for **Ic** the binding energy is higher than for **Ib**. The attractive part of correlation energy is the dispersion interaction, while in HF binding energy attractive terms are electrostatic charge transfer and polarization [23]. It is shown that correlation stabilization is most important for **Ia**, where it represents most of the binding energy; it is less important for conformers where positive charged nitrogen is involved in the binding. It is clearly seen that higher binding energy for **Ib**+ compared with **Ic**+ is due to electrostatic interactions and not correlation stabilization (correlation stabilization is higher for **Ic**+). A great difference in correlation stabilization between **Ib** and **Ic** is due their conformations. As shown in Figures 1 and 2, stacking in **Ic** π–π involves an anthracene unit and three benzene rings, whereas the **Ib** anthracene fragment does not participates in π–π interactions. Since the main contribution to the stabilization energy in the case of π–π stacking is dispersion conformer **Ic** has higher correlation stabilization. To separate different contributions to the interaction energy in different states of the molecular "shuttle," the binding energy of various model systems was calculated at the same theoretical level as the molecular "shuttle." Figure 5 and Table III show model complexes and their binding energies, respectively. Interactions in complexes **M1**, **M2**, **M3**, **M4**, **M5**, and **M6** model NH$\cdots$O interaction in conformer **Ia**, $^+$NH$\cdots$O interactions in **Ia**+, O$\cdots$HCN$^+$ interactions in **Ia**+, O$\cdots$HCN$^+$ interactions in **Ib**+ and **Ic**+, π–π stacking interactions in **Ib**+ and **Ic**+ and π–π stacking interactions in **Ia**+ and **Ia**, respectively. One can distinguish two types of interactions; one type is $^+$NCH$\cdots$O and O$\cdots$HN$^+$ interactions, which are mostly electrostatic and the correlation stabilization represents less than 30% of total binding energy. Another type is π–π stacking, where correlation stabilization is the most important part of stabilization. Conformer **Ia**+ is stabilized by two $^+$NH$\cdots$O bonds (−36.4 kcal/mol) and π–π stacking (−14.3 kcal/mol) giving a sum of −50.7 kcal/mol. The rest of the binding energy comes from $^+$NCH$\cdots$O bond with shortest H$\cdots$O distance of 2.26 Å giving a total binding energy of −62.3 kcal/mol, close to −62.1 calculated for conformer **Ia**+ (Table II). In a similar way, one can estimate different contributions to the

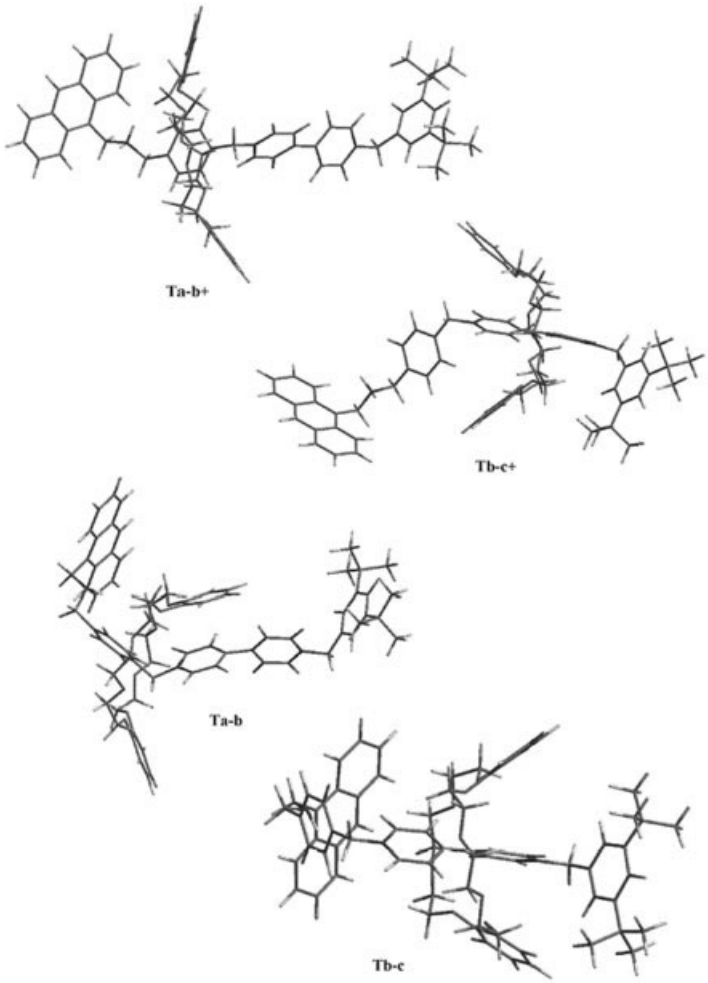

FIGURE 4. "Transition state" structures located for the shuttling process at BHandHLYP/6-31G* level of theory.

binding energies for conformers **Ib**+ and **Ic**+ In those cases, π–π stacking interactions will be of −22 kcal/mol (two times binding energy of complex M5) where a great deal of binding is due to CT interactions. The rest of the binding energy corresponds to three $^{+}$NCH· · ·O bonds, giving a total of −59.5 kcal/mol, very close to the binding energies of −59.8 and −56.6 kcal/mol for conformers **Ib**+ and **Ic**+, respectively. As seen in the analysis for conformers **Ib**+ and **Ic**+ π–π stacking is more important source of stabilization compared with **Ia**+ comprising more than 40% of total stabilization energy. In this case, CT is involved.

In the case of deprotonated conformers **Ia**, **Ib**, and **Ic** situation changes. The binding energy of **Ia** is due to mostly correlation stabilization coming from π–π stacking −14.3 kcal/mol and one NH· · ·O H-bond giving a total of −18.9 kcal/mol

TABLE II

Gas phase binding energies (kcal/mol) of translational conformers at LMP2/6-31G*//BH and HLYP/6-31G* (LMP2) and HF/6-31G*//BH and HLYP/6-31G* (HF) levels.*

Complex	LMP2	HF	ΔE_{corr}[a]	LMP2(solv)
Ia+	−62.1	−40.6	−21.5	−21.7
Ib+	−59.8	−38.8	−21.0	−17.1
Ic+	−56.6	−32.3	−24.3	−11.9
Ia	−18.3	−2.5	−15.8	5.7
Ib	−46.6	−42.7	−3.9	−7.5
Ic	−48.8	−35.3	−13.5	−12.3

* LMP2/6-31G*//BH and HLYP/6-31G* binding energy in acetone [LMP2(solv)].

[a] Difference between LMP2 and HF binding energy.

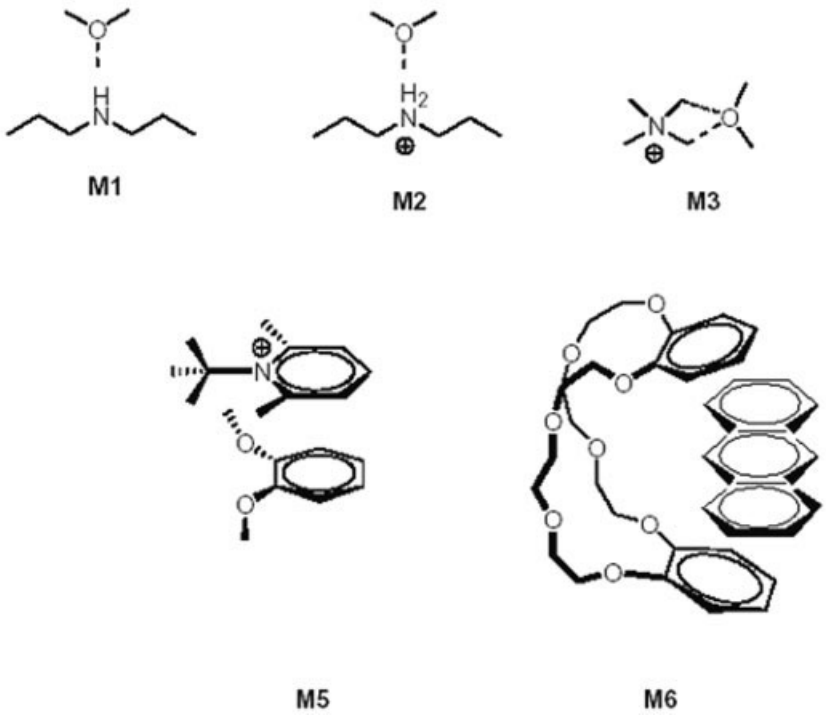

FIGURE 5. Structures of model complexes for modeling of intermolecular interactions in translational conformers of molecular "shuttle" I.

that is close to −18.3 kcal/mol. Analysis of Table II shows that lower binding energies of conformers **Ib** and **Ic** compared with **Ib**+ and **Ic**+ are due to smaller correlation stabilization. Since correlation stabilization comes mostly from π–π stacking interactions, therefore π–π stacking in conformers **Ib** and **Ic** is less effective compared with **Ib**+ and **Ic**+. As shown in Figures 1 and 2, due to rather bent conformation of "finger" fragment in conformers **Ib** and **Ic** average distances between planes of aromatic fragments increase by some 0.5 A compared with **Ib**+ and **Ic**+. Since dispersion interactions are short range ones this causes noticeable debilitating of correlation stabilization.

Since the major contribution to the binding energy comes from electrostatic interactions, it is reasonable to suggest that the binding energy decreases in solvents, as electrostatic interactions make an important contribution to total binding energy. Actually, this fact was confirmed both experimentally [24] and theoretically [9]. The relative order of the binding energies in solution coincides with that for gas phase; however, it is greatly decreased.

TABLE III

Gas phase binding energies (kcal/mol) of model complexes at LMP2/6-31G*//BH and HLYP/6-31G* (LMP2) and HF/6-31G*//BH and HLYP/6-31G* (HF) levels of theory.

Complex	LMP2	HF	ΔE_{corr} [a]
M1	−4.6	−1.7	−2.9
M2	−18.2	−14.8	−3.4
M3	−11.6	−8.5	−3.1
M4	−12.5	−9.9	−2.6
M5	−11.0	−3.7	−3.3
M6	−14.3	−0.6	−13.7

[a] Difference between LMP2 and HF binding energy.

Conclusions

Calculations at the LMP2/6-31G*//BHandHLYP/6-31G* level reproduce correctly experimental observations for molecular "shuttle" **I**. The theoretical study shows that the $Bpym^{2+}$ station consists of two "substations" separated by a barrier, and the relative energies of two "substations" depend on

the state of $^{+}NH_2$–NH station showing that in this molecular "shuttle" exist mutual influence of the "stations." Thus, strong electron withdrawing effect of $+NH_2$ group decreases relative energy of **Ib**+ compared with **Ic**+, while **Ic** is more stable than **Ib**. Conformer **Ia**+ is stabilized by two $^{+}NH\cdots O$, one $^{+}NCH\cdots O$ bonds and π–π stacking, while conformers **Ib**+, **Ic**+, **Ib**, and **Ic** are stabilized by three +NCH-O bonds and π–π stacking involving CT interaction between catechol and $Bpym^{2+}$ fragments. The binding energy of conformer **Ia** is mostly due to π–π stacking.

References

1. Raymo, F. M.; Stoddart, J. F. Chem Rev 1999, 99, 1643.
2. Ashton, P. R.; Ballardini, R.; Balzani, V.; Baxter, I.; Credi, A.; Fyfe, M. C .T.; Gandolfi, M. T.; Gomez-Lopez, M.; Martinez-Díaz, M.-V.; Piersanti, A.; Spencer, N.; Stoddart, J. F.; Venturi, M.; White, A. J. P.; Williams, D. J. J Am Chem Soc 1998,120, 11932.
3. (a) Jang, S. S.; Jang, Y. H.; Kim, Y-H.; Goddard, W. A., III; Flood, A. H.; Laursen, B. W.; Tseng, H.-R.; Stoddart, J. F.; Jeppesen, J. O.; Choi, J. W; Steuerman, D. W.; Delonno, E.; Heath, J. R. J Am Chem Soc 2005,127, 1563; (b); Deng, W-Q.; Muller, R .P.; Goddard, W. A., III. J Am Chem Soc 2004, 126, 13562.
4. Grabuleda, X.; Ivanov, P.; Jaime, C. J Phys Chem B 2003, 107, 7582.
5. Grabuleda, X.; Ivanov, P.; Jaime, C. J Org Chem 2003, 68, 1539.
6. Grabuleda, X.; Jaime, C. J Org Chem 1998, 63, 9635.
7. Frankfort, L.; Sohlberg, K. J Mol Struct (Theochem) 2003, 621, 253.
8. Raymo, F. M.; Bartberger, M. D.; Houk, K. N.; Stoddart, J. F. J Am Chem Soc 2001 123, 9264.
9. Romero, C.; Guadarrama, P.; Fomine, S. J Mol Mod 2005, 12, 85.
10. Jaguar 6.0; Schrödinger, LLC; Portland, OR, 2005.
11. Reyes, A.; Tlenkopatchev, M. A.; Fomina, L.; Guadarrama, P.; Fomine, S. J Phys Chem A 2003, 107, 7027.
12. Huang, N.; MacKerell, A. D., Jr. J Phys Chem A 2002, 106, 7820.
13. Schu1tz, M.; Rauhut, G.; Werner, H-J. J Phys Chem A 1998, 102, 5997.
14. Tannor, D. J.; Marten, B.; Murphy, R.; Friesner, R. A.; Sitkoff, D.; Nicholls, A.; Ringnalda, M.; Goddard, W. A., III; Honig, B. J Am Chem Soc 1994, 116, 11875.
15. Marten, B.; Kim, K.; Cortis, C.; Friesner, R. A.; Murphy, R. B.; Ringnalda, M.; Sitkoff, D.; Honig, B. J Phys Chem 1996, 100, 11775.
16. Barone, V.; Cossi, M.; Tomasi, J. J Chem Phys 1997, 107, 3210.
17. Pomeli, C. S.; Tomasi, J.; Sola, M. Organometallics 1998, 17, 3164.
18. Cacelli, I; Ferretti, A. J Chem Phys 1998, 109, 8583.
19. Creve, S.; Oevering, H.; Coussens, B. B. Organometallics 1999, 18, 1967.
20. Bernardi, F.; Bottoni, A.; Miscone, G. P.; Organometallics 1998, 17, 16.
21. Cantrill, S. J.; Pease, A. R.; Stoddart, J. F. J Chem Soc Dalton Trans 2000, 3715.
22. Kaplan, I. G; Roszak, S.; Leszczynski, J. J Chem Phys 2000, 113, 6245.
23. Kitaura, K; Morokuma, K. Int J Quantum Chem 1976, 10, 325.
24. Ashton, P. R.; Campbell, P. J.; Chrystal, E. J. T.; Glink, P. T.; Menzer, S.; Philp, D.; Spencer, N.; Stoddart, J. F.; Tasker, P. A.; Williams, D. J. Angew Chem Int Ed Engl 1995, 34, 1865.